Study of Electronic and Molecular Properties of Poly (3-Octylthiophene-2,5 diyl) Polymer using Density Functional Theory (DFT) And Time-Dependant Density Functional Theory (TD-DFT)

Hassana Muhammad Shuwa[1*], Mansur Said[2] and A. S. Gidado[3]

[1]*Yobe State University Damaturu, Faculty of Sciences, Physics Department, Yobe, Nigeria.*
[2]*Yusuf Maitama Sule University, Faculty of Sciences, Physics Department, Kano, Nigeria.*
[3]*Bayero University Kano, Faculty of Physical Sciences, Physics Department, Kano, Nigeria.*

Authors' contributions

Article Information

Original Research Article

ABSTRACT

Poly(3-octylthiophene-2,5-diyl) denoted as P3OT with a chemical formula $(C_{12}H_{18}S)n$ is an alkylthiophene based conductive polymer with high electroluminescence that is soluble in most of the organic solvents. P3OT is a promising material for applications in solar cells, light-emitting diodes, displays, and other optoelectronic devices due to their processability, flexibility, and low production cost. In this work, DFT and TD-DFT methods were used to investigate the molecular and electronic properties of P3OT in a vacuum (gas phase). The effect of solvent was also investigated using different models such as Polarisable Continuum Model (PCM), Continuum polarisable continuum model (C-PCM), and Integral Equation Fourier Polarisable continuum model

---

Corresponding author: Email: hassanamuhdshuwa@gmail.com;

(IEFPCM) with Chloroform, Tetrahydrofuran (THF), and Toluene as solvents. Gaussian 09 program was used for all the calculations at the DFT/B3LYP/6-311+G(d) level of theory. The results obtained for the molecular geometry show that the lowest average value of bond length in the vacuum and the medium are *1.08311Å* and *1.0830Å* respectively. The HOMO, LUMO and Energy-gap calculated in the vacuum are obtained as *-6.44eV,-3.63eV* and *2.81eV* respectively while the results obtained in medium show a little effect on the HOMO, LUMO and energy gap for all the solvents. The energy gap obtained is compared with the one in literature (*2.51eV*).This indicates that the reported energy-gap leads by *0.3eV*. From the UV-VIS spectrum, the excitation energy and oscillator strength were found to be *948.46nm* and *0.0015* in the vacuum, while in the medium, the presence of solvents increase the excitation energy in the range *950.10-956.07nm* and oscillator strength in the range *0.0020-0.0022*. The open-circuit voltage was calculated theoretically. The result shows that the open-circuit voltage was found to be *2.711eV*, this value is sufficient for possible electron injection from the molecule to the conduction band of ICBA(Indene-C60-bisadduct). Thus, it can be concluded that P3OT shows high stability and low reactivity in a chemical reaction, and due to its strong absorption properties in both a vacuum and a medium, it can be used for solar cell application.

1. INTRODUCTION

Since their discovery, organic materials based on conjugated polymers have attracted the interest of many scientists in the world, due to their unique electrical and optical properties, reasonable chemical stability, and easy processability. These unique properties of conjugated polymers enable the development of several electronic devices, such as organic light emitting diodes, organic solar cells, transistors, sensors and so on [1]. Polythiophene and its derivatives have been considered one of the most promising conjugated polymers due to their high stability, ease of structural modification, and controllable optical and electrochemical properties. In the beginning, the applications of non substituted Polythiophene were very limited because of its insolubility in many organic solvents, due to its extended conjugated structure. Furthermore, the alkyl chain has been incorporated into the thiophene units to obtain a functional monomer able to yield soluble polymers. The poly(3-alkylthiophenes) resulted to be highly processable conducting polymers whose solubility allowed their full characterization by spectroscopic method [2]. Poly (3-Octylthiophene-2,5 diyl) belongs to the poly(3-alkylthiophene) family, it has a molecular formula $(C_{12}H_{18}S)n$. P3OT has been extensively studied as promising materials for applications in solar cells, light-emitting diodes, displays, or other optoelectronic devices due to their processability, flexibility, and low production costs. On the other hand, many important aspects of the electronic and optical properties of these materials are still not fully resolved [3].

In 2011, the investigation of the HOMO and LUMO of poly(3-octylthiophene-2,5 diyl) an[6,6]-phenyl C61-butyric acid 3-ethylthiophene ester using cyclic voltammetry methods were reported. Platinum working electrode, platinum counter electrode, and SCE reference electrodes were used in conducting the experiments. The HOMO, LUMO, and band-gap energy of P3OT are 5.59eV,3.76eV and 1.83eV while the HOMO, LUMO, and band-gap energy of PCBE are 5.87eV, 3.91eV, and 1.96eV respectively [4]. Abu-Abdeen et al. also reported the effect of CNTs on the optical, electrical and mechanical properties of poly(3-octylthiophene-2,5 diyl). The result of their investigation showed that the addition of CNTs to the P3OT molecule decreases the value of the band gap energy from 2.74eV to 2.51eV[3]. In 2013, the light-emitting assistance effect of perylene on polymer electrochemiluminescence (ECL) device was also reported by Tatsuya et al, using poly (3-octylthiophene 2,5 diyl) molecule. The HOMO, LUMO and band-gap energy were reported as -4.97eV, -2.62eV, and 2.35eV respectively[5]. Very recently, spectrophotometry and ellipsometry methods were reported by Natalia et al. to investigate the basic optical parameters and electronic structure of conjugated polymer. Their report discovered that P3HT and P3OT had band-gap energies of 2.43eV and 2.51eV respectively [6].

Also, DFT and TD-DFT studies have been applied for several organic molecules such as Cyanidin [7], Phenylenevinylene [8], Aceantraquinoxaline [9], Triphenylamine [10], Thionopyrazine and thiophene [11], thiophene,

and benzene[12] for solar cell applications. DFT-based calculations have been significant in understanding the electronic properties of different systems on an atomic scale therefore performing studies using DFT will aid experimentalists in the design, prediction, and functionalization of different materials necessary for a specific application.

In this work, the study of the molecular and electronic properties of poly (3-octylthiophene-2,5-diyl)(P3OT) was reported, using DFT and TD-DFT methods. The study covered building P3OT, testing for stability, optimizing the structure with B3LYP at different basis sets, calculating the HOMO, LUMO and energy gap. The work further looked into some properties of P3OT that were not reported in the literature such as ionization potential, electron affinity, infrared spectrum, and UV Visible spectrum. The solvent effect was also investigated and reported. The open-circuit voltage was calculated theoretically using P3OT (Donor) and ICBA (Acceptor).

2. THEORETICAL BACKGROUND

2.1 Density Functional Theory

Density functional theory is a variational method that is presently the most successful approach to compute the electronic structure of matter. Its applicability ranges from atoms, molecules, and solids to nuclei, quantum, and Classical fluids. The density functional theory is derived from the N-particle Schrodinger equation and is expressed in terms of the density distribution of the ground state and the single-particle wave function. DFT reduces the calculations of the ground- state properties of systems of an interacting particle exactly to the solution of single-particle Hartree-type equations. This is why it has been most useful for systems of very many electrons [13]. The entire field of Density Functional Theory rests on two fundamental mathematical theorems by Hohenberg and Kohn:

The first theorem state that the ground state electron density uniquely determines the electronic wave function and hence all ground-state properties of an electronic system.

$$\rho(r) = \psi^2(r) \qquad (1)$$

$$E = E_{in} + E_{en} + \frac{1}{2} \int \rho(r) dr \int \frac{\rho(r)'}{r-r'} dr + E_{xc} \qquad (2)$$

The second theorem states that: the energy of an electron distribution functional reaches a minimum in correspondence to the actual ground-state electron density [14].

Since $\psi' \neq \psi$

$$E[\boldsymbol{n}] = \langle \psi' H \psi' \rangle > \langle \Psi_0 H \Psi_0 \rangle \qquad (3)$$

2.2 Vibrational Frequency

The vibrational frequencies are calculated with the following equations [15]:

$$V_{ij} = \frac{1}{\sqrt{m_i m_j}} \left(\frac{\partial^2 v}{\partial_{\alpha i} \partial_{\alpha j}} \right) \qquad (4)$$

Where V_{ij} is the Hessian matrix, m_i refers to the mass of atom I, and $\partial_{\alpha i}$ is a displacement of atom i in the x-,y- and z- direction.

$$UV = \lambda U \qquad (5)$$

Where U is a matrix of eigenvectors and λ is a vector of Eigen values, and

$$\lambda_k = (2\pi v_k)^2 \qquad (6)$$

Where λ_k is the Kth eigenvalue and v_k is the Kth vibrational frequency. The infrared intensities can be computed with the equation [15].

$$\frac{\partial E_{SCF}}{\partial f \partial a} = 2 \sum_i^{d.o} h_{ij}^{fa} + 4 \sum_i^{d.o} \sum_j^{all} U_{ji}^a h_{ij}^f \qquad (7)$$

$$h_{ij}^{fa} = \sum_{\mu v}^{AO} C_\mu^{i0} C_v^{i0} \left(\frac{\partial^2 h_{\mu v}}{\partial f \partial a} \right) \qquad (8)$$

Where E_{SCF} is the self-consistent field energy, f is the electric field, α is the nuclear coordinate, h_{UV} is the one-electron atomic orbital integral, U^α is related to the derivative of the molecular orbital coefficient with respect to α by

$$\frac{\partial C_U^i}{\partial \alpha} = \sum_m^{all} U_{mi}^\alpha C_u^{m.o} \qquad (9)$$

2.3 Global Reactivity Descriptors

The global reactivity descriptors are described as [16-17]:

The Chemical potential is defined as

$$\mu = -\chi \qquad (10)$$

The absolute electronegativity (χ) is given by the relation;

$$\chi = \frac{IP+EA}{2} \qquad (11)$$

The global hardness (η) and global softness(S) are defined as;

$$\eta = \frac{IP-EA}{2} \qquad (12)$$

$$S = \frac{1}{2}\eta \qquad (13)$$

The electrophilicity (ω) can be calculated using the chemical potential and the chemical hardness;

$$\omega = \frac{\mu^2}{2\eta} \qquad (14)$$

The energy corresponding to HOMO represents the ionization potential and LUMO corresponds to the electron affinity of the molecule. Using Koopmans theorem;

Ionization Potential (IP) $= -E_{HOMO}$

Electron Affinity (EA) $= -E_{LUMO}$

2.4 Open-Circuit Voltage (V_{OC})

The maximum open-circuit voltage (V_{OC}), is an important photovoltaic parameter that can be determined theoretically by the difference between the highest occupied molecular orbital (HOMO) of the donor and the lowest unoccupied molecular orbital (LUMO) of the electron acceptor. The theoretical value of V_{OC} has been calculated from the expression [8];

$$V_{OC} = E_{HOMO}^{Donor} - E_{LUMO}^{Acceptor} - 0.3 \qquad (15)$$

3. MATERIALS AND METHODS

The molecular structure of poly(3-octylthiophene-2,5-diyl)(P3OT) was built using Gaussview, which is a graphical user interface design for preparing input files for submission to Gaussian and to examine graphically the output that Gaussian produces. The built structure was used at restricted Hartree Forck (RHF) method with STO-3G basis set, in order to check the stability of the studied molecule. The stable structure was later used as an input for calculating the ground state geometry optimization at the level of Density Functional Theory with Becke's three parameters and the Lee-Yang-Parr gradient

correlation potential (B3LYP) using different basis sets: STO-3G,3-21G,6-31G, and 6-311G. This procedure was performed to obtain the lowest minimum energy potential value. All the parameters were allowed to relax and each calculation converged to an optimized geometry that corresponded to true energy minima. The geometry optimization was further carried out by adding the polarization and diffuse functions to the basis sets 6-311G: DFT/B3LYP/6-311+G(d). This optimized geometry was then used as the starting geometry to compute the HOMO, LUMO, energy-gap, ionization potential, and electron affinity of the studied molecule. At the same level of theory, the vibrational frequency (IR spectrum) was also computed using the optimized geometry. The Vibrational frequency analysis was performed by computing the Hessian matrix and the force constants for all the normal modes of the molecule. The Frequency calculations involved computing the energy of the input structure, it then went on to compute the frequencies and intensities of each spectral line of the studied molecule. IRPAL 2.0 was used for the interpretation of the spectra. No imaginary frequencies were obtained which indicate the stability of the molecule was achieved. The optimized geometry was also used for the non-equivalent TD-DFT/B3LYP/6-311+G(d) method for calculating the UV-Vis spectrum. The spectrum was plotted using GaussSum 3.0 Software. The solvent effects were implicitly considered for all the calculations at the same level of theory in the default (PCM), C-PCM, and IEFPCM models, using different solvents: Chloroform, Toluene, and THF. All the calculations were carried out using the window version of the Gaussian 09 software package [18].

4. RESULTS AND DISCUSSION

4.1 Stability Check

From the stability check, it was observed that there was an appearance of some partial bond in the thiophene ring, which shows that the structure was tightly stable and the bonding between the atoms are strong. The energies obtained for single stability and optimized-stability are -23190.16eV and -23193.05eV. This indicates that the structure is approaching ground level.

4.2 Geometry Optimization

The main aim of geometry optimization is to determine the atomic arrangement that makes a

molecule stable. In this study, the molecular structure of P3OT was fully optimized in the ground state, using density functional theory at B3LYP with different basic sets of STO-3G, 3-21G, 6-31G, and 6-311G. The results obtained for geometry optimization are presented in Table 1.0, the minimum amount of energy and the time taken to complete each optimization are listed in the table. From the result, the basis sets 6-311G has the lowest minimum energy value of -866.0773a.u (- 23566.8294eV).

4.3 Optimized Bond Lengths

The optimized bond lengths and bond angles of the studied molecule calculated at DFT/B3LYP with 6-311+G(d) basis sets, in a vacuum and a medium are listed in Table 2(a). According to molecular orbital (MO) theory, a covalent bond between two atoms is formed by the overlap of their atomic orbital. During overlapping, when the force of attraction between the atoms is balanced by the force of repulsion between the nuclei of two atoms, the equilibrium distance between the two atomic nuclei is called bond length [19]. The result obtained shows that the lowest average value of bond lengths in a vacuum and a medium are 1.08311Å and 1.0830Å. This indicates that these values are a bit higher in a vacuum than in medium, which implies that the bonds will be slightly stronger in medium. It was observed that the bonds C_2-H_6, C_{28}-H_{30}, C_{28}-H_{31}, and C_{28}-H_{29} between carbon and hydrogen atoms at the indicated positions have the lowest values of

bond lengths ranging from 1.08311Å – 1.09488Å in vacuum and 1.08308Å – 1.09494Å in a medium. These are the strongest bonds and have the largest values of bond energy in P3OT molecule which cannot be broken easily. On the other hand, the bonds C_2-C_7, C_{25}-C_{28}, C_7-C_{10} and C_{22}-C_{25} carbon and carbon atoms have the highest value of bond lengths ranging from 1.50189Å – 1.53253Å in a vacuum and 1.50178Å – 1.53256Å in a medium. These are the weakest bond and have the lowest value of bond energies; less amount of energy is required to break them.

4.4 Optimized Bond Angles

The bond angle is the internal angle between the orbital-containing electron pairs in the valence shell of the central atom in a covalent molecule [20]. From the result obtained, it was observed that the angle between H_8-C_7-H_9, H_{20}-C_{19}-H_{21}, H_{18}-C_{16}-H_{17}, and H_{26}-C_{25}-H_{27} have the lowest values of bond angles in the range 105.429 - 105.815° in a vacuum and 105.449 – 105.923° in a medium. While the bonds C_3-C_2-H_6, C_1-C_2-H_6, C_{16}-C_{19}-C_{22}, and C_{13}-C_{16}-C_{19} have the highest value of bond angles in the range of 129.754 - 114.845° in a vacuum and 129.663-114.814° in a medium. This shows that the values obtained in a vacuum are higher than the ones obtained in a medium by 0.091°.

Fig.1. Structure of Poly (3-octylthiophene -2,5-diyl) (a) Initial (built) (b) Stable structure (c) optimized structure

Table 1. Optimization at B3LYP with different basis sets (1a.u =27.211eV)

Basic sets	Energy (a.u)	Energy (eV)	Time (minute)
STO-3G	-856.0791	-23294.7683	12.40
3-21G	-861.5850	-23444.5894	16.19
6-31G	-865.9536	-23563.4634	19.30
6-311G	-866.0773	-23566.8294	21.10

Table 2(a). Optimized bond lengths (Å) of P3OT in Vacuum and Medium at DFT/B3LYP/6-311+G(d)

S/N	Bonds	Bond length(Å) Vacuum	Bond length(Å) Medium
1	C_1-S_5		1.68835
2	C_1-C_2	1.37439	1.37535
3	C_2-C_3	1.42016	1.42013
4	C_3-C_4	1.37808	1.37833
5	C_4-S_5	1.68827	1.68801
6	C_2-H_6	1.08311	1.08308
7	C_3-C_7	1.50189	1.50178
8	C_7-H_9	1.09805	1.09780
9	C_7-H_8	1.09804	1.09779
10	C_7-C_{10}	1.53076	1.53069
11	C_{10}-H_{12}	1.09703	1.09712
12	C_{10}-H_{11}	1.09689	1.09695
13	C_{10}-C_{13}	1.53295	1.53312
14	C_{13}-H_{15}	1.09855	1.09841
15	C_{13}-H_{14}	1.09630	1.09619
16	C_{13}-C_{16}	1.53327	1.53325
17	C_{16}-H_{17}	1.09720	1.09721
18	C_{16}-H_{18}	1.09823	1.09825
19	C_{16}-C_{19}	1.53604	1.53613
20	C_{19}-H_{21}	1.09836	1.09836
21	C_{19}-H_{20}	1.09730	1.09731
22	C_{19}-C_{22}	1.53337	1.53343
23	C_{22}-H_{24}	1.09873	1.09871
24	C_{22}-H_{23}	1.09671	1.09668
25	C_{22}-C_{25}	1.53253	1.53256
26	C_{25}-H_{26}	1.09732	1.09733
27	C_{25}-H_{27}	1.09736	1.09737
28	C_{25}-C_{28}	1.53040	1.53055
29	C_{28}-H_{29}	1.09488	1.09494
30	C_{28}-H_{30}	1.09388	1.09397
31	C_{28}-H_{31}	1.09485	1.09492

4.5 Frontier Molecular Orbitals

The highest occupied molecular orbital energy (HOMO) and the lowest unoccupied molecular orbital energy (LUMO) are very important quantum chemical parameters. These orbitals, also called the frontier orbitals determine the way the molecule interact with other species. HOMO acts as an electron donor while LUMO acts as an electron acceptor. Molecular orbital's when viewed in a qualitative graphical representation can provide insight into the nature of reactivity and some of the structural and physical properties of molecules. The positive and negative phases are represented in red and green colours respectively [21].

The HOMO-LUMO gap (energy gap), which is the difference in energy between the HOMO and LUMO, is an important stability index. A large HOMO-LUMO gap implies low chemical reactivity because it hinders adding electrons to a high lying LUMO or extracting electrons from a low lying HOMO and prevents the formation of the activated complex of any further reaction [22]. The HOMO-LUMO gap is defined as;

$$E_g = E_{LUMO} - E_{HOMO}$$

The results of the E_{HOMO}, $E_{LUMO,}$ and Energy gap obtained in a vacuum and medium are listed in Table 3(a) and (b).

4.6 Global Chemical Descriptors

Ionization potential is defined as the amount of energy needed to remove an electron from a molecule. High ionization energy indicates high stability and chemical inertness, while small ionization energy indicates the high reactivity of

atoms and molecules. The electron affinity is the energy released when an electron is added to a neutral molecule. A molecule with high electron affinity tends to take electrons easily [16]. The chemical potential (μ) measures the escaping tendency of an electron and it can be associated with the molecule's electronegativity then, as μ becomes more negative, it is difficult to lose an electron but easier to gain one. The electronegativity(χ) represents the ability of a molecule to attract electrons. The hardness and softness are useful for understanding the behaviour of a chemical system. A hard molecule has a large energy-gap and a soft molecule has a small energy-gap, therefore soft molecule will be more polarized. The results obtained for the global chemical descriptors are listed in Table 4.0

**Table 2(b). Optimized bond angles (°) of P3OT in Vacuum and Medium at DFT/B3LYP/6-311+G(d)**

S/N	Bonds	Bond Angle in Vacuum	Bond Angle in Medium
1	C_1-C_2-H_6	123.124	123.166
2	C_3-C_2-H_6	129.754	129.663
3	C_3-C_7-H_9	108.860	108.810
4	C_3-C_7-H_8	108.848	108.792
5	H_8-C_7-H_9	105.429	105.449
6	H_9-C_7-C_{10}	109.762	109.802
7	C_7-C_{10}-H_{12}	109.276	109.322
8	H_{12}-C_{10}-H_{11}	106.007	106.101
9	C_7-C_{10}-C_{13}	113.109	113.045
10	C_{10}-C_{13}-H_{14}	109.021	108.983
11	H_{14}-C_{13}-H_{15}	106.011	106.077
12	H_{15}-C_{13}-C_{16}	109.123	109.130
13	C_{13}-C_{16}-C_{19}	114.845	114.814
14	H_{18}-C_{16}-H_{17}	105.747	105.807
15	H_{17}-C_{16}-C_{19}	108.609	105.605
16	C_{16}-C_{19}-H_{20}	108.503	108.501
17	C_{16}-C_{19}-H_{21}	109.231	109.221
18	H_{20}-C_{19}-H_{21}	105.706	105.766
19	C_{16}-C_{19}-C_{22}	114.968	114.951
20	C_{19}-C_{22}-H_{24}	109.201	109.184
21	H_{24}-C_{22}-H_{23}	105.873	105.923
22	H_{23}-C_{22}-C_{25}	108.847	108.850
23	C_{22}-C_{25}-H_{26}	109.302	109.292
24	C_{22}-C_{25}-H_{27}	109.245	109.237
25	H_{26}-C_{25}-H_{27}	105.815	105.869
26	C_{22}-C_{25}-C_{28}	113.342	113.328
27	H_{27}-C_{25}-C_{28}	109.425	109.417
28	C_{25}-C_{28}-H_{30}	111.554	111.540
29	C_{25}-C_{28}-H_{31}	111.369	111.333
30	H_{31}-C_{28}-H_{29}	107.370	107.403
31	H_{29}-C_{28}-H_{30}	107.470	107.501

Table 3(a). E_{HOMO}, E_{LUMO} and Band Gap(E_g) of P3OT(Donor) and ICBA(acceptor) at DFT/B3LYP/6-311+G(d) computed in vacuum

Molecule	E_{HOMO}(eV)	E_{LUMO}(eV)	E_g(eV)	Previous work [6]
P3OT	-6.44	-3.63	2.81	2.51
ICBA	-5.96	-3.43	2.53	

Table 3(b). E_{HOMO}, E_{LUMO}, and Energy gap of P3OT computed at DFT/B3LYP/6-311+G(d) in a Medium

Model	C-PCM			PCM			IEFPCM		
Solvent	HOMO	LUMO	Eg	HOMO	LUMO	Eg	HOMO	LUMO	Eg
Chloroform	-6.529	-3.706	2.822	-6.515	-3.696	2.819	-6.515	-3.696	2.819
THF	-6.539	-3.716	2.823	-6.528	-3.707	2.820	-6.528	-3.707	2.820
Toluene	-6.504	3.684	2.820	-6.484	-3.670	2.814	-6.484	-3.670	2.814

(a) HOMO

LUMO

(b) HOMO

LUMO
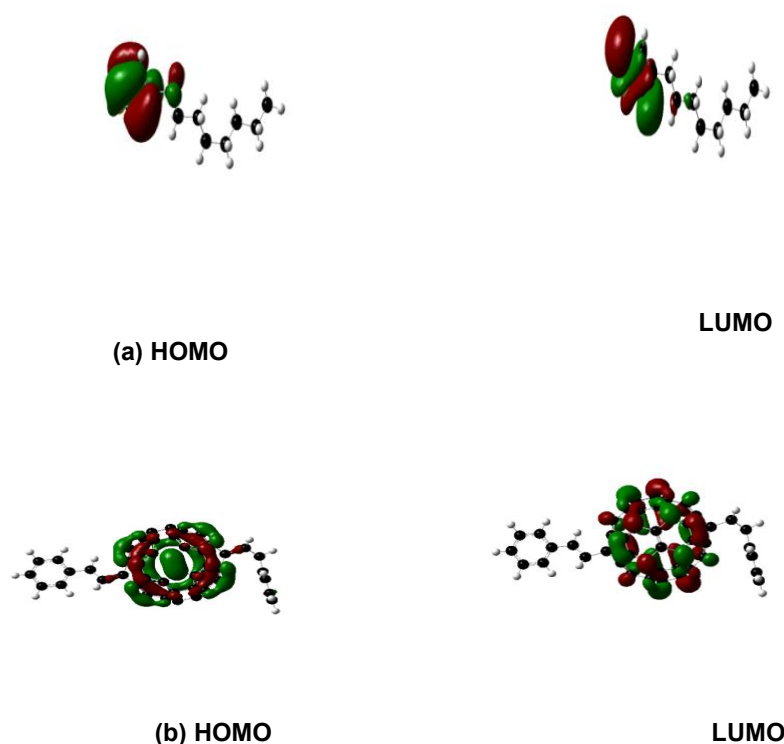
Fig. 2. Molecular orbital of (a) poly (3-octylthiophene- 2,5-diyl) (P3OT) (b) Indene C_{60} Bisadduct (ICBA)

4.7 UV-Visible Spectrum

UV-VIS spectrum is due to the interaction of electromagnetic radiation in the UV-Visible region with molecules, ions, or complexes. It forms the basis analysis of different substances such as inorganic, organic and bio-molecules. On the other hand, how the absorption of a new material matches with the solar spectrum is an important factor for the application as a photovoltaic material and a good photovoltaic material should have broad and strong visible absorption characteristics [23]. In this study, the UV-Visible spectrum was calculated from the optimized geometry of the studied molecule in a vacuum and a medium using TD-DFT at the B3LYP/6-311+G(d) level of theory. The absorption spectrum was presented as oscillator strength against excitation energy as shown in Fig 3(a) and (b), GaussSum 3.0 was used to plot the spectrum [24]. The results obtained in vacuum show that the studied molecule has maximum excitation energy of 948.46nm and oscillator strength of 0.0015. These indicate that P3OT is a good photovoltaic material due to its strong absorption character.

In the medium, the excitation energy and oscillator strength are listed in Table 5 using different models: PCM, C-PCM, and IEFPCM. With solvents: Chloroform, Tetrahydrofuran(THF),and Toluene. The results obtained show that due to the solvent effect, there was an increase in the excitation energy and oscillator strength. The excitation energies were in the range of 950.10-956.07nm for PCM and IEFPCM, and 951.36-955.89nm, Toluene has the highest value of excitation energy for all the models. While the oscillator strength was found to be 0.0020 for PCM and IEFPCM and 0.0022 for the C-PCM model.

4.8 Infrared Spectrum

Infrared spectroscopy is the study of how molecules absorb infrared radiation and thus convert it to heat. Thus an IR spectrum is the study of the interaction of infrared light with matter. When a molecule absorbs infrared radiation, its chemical bond vibrates and may either be stretched, contracted, or bend [25]. From the result obtained, the molecule has 31 atoms and 87 normal modes of vibrations, no imaginary frequency was found in both vacuum and medium. This shows that the molecule was stable. The spectrum was plotted as IR against frequency in Figure 4(a) and (b). In a vacuum, the most intense frequency was found to be *3062cm^{-1}* at an intensity of *111.70km/mol*, at this frequency there is a medium =C-H stretch, strong (broad) dimer OH, and small Ar-H stretch mode of vibrations were observed. The second most intense frequency was found to be *3080cm^{-1}* at an intensity of *87.6000km/mol*. At this frequency there is a medium =CH stretch, strong

(broad) dimer OH and small Ar-H stretch mode of vibrations were observed. The third most intense frequency was found to be 3010cm^{-1} at an intensity of *70.4199km/mol*. At this frequency, there is a strong (broad) dimer OH and a small Ar-H stretch. IR PAL 2.0 was used to interpret these frequencies [26].

In the medium, the most intense frequency was found to be 3058.66cm^{-1} at an intensity of *190.6917km/mol.* At this frequency, medium =CH stretch, strong (broad) dimer OH, strong (broad)dimer OH, and Ar-H stretch were observed. The second most intense frequency was *3013cm^{-1}* at an intensity of *127.6619km/mol*. At this frequency, strong (broad) dimer OH, strong (broad) dimer OH, and small Ar-H stretch were observed. The third most intense frequency was *501cm^{-1}* at an intensity of *101.4608km/mol*. At this frequency, small C-Br stretch and Wagg S-S disulfide asymmetry mode of vibrations were observed.

4.9 Open-circuit Voltage (V$_{OC}$)

The open-circuit voltage of an organic solar cell is related to the difference between the HOMO of the donor and the LUMO of the electron acceptor, taking into account the energy loss during photo charge generation [22]. The theoretical value of V$_{OC}$ has been calculated using equation (15), the value obtained was *2.7119eV*. This value is sufficient for possible efficient electron injection; therefore the studied molecule can be used for organic solar cell application.

Table 4. Quantum chemical descriptors of P3OT calculated at DFT/B3LYP/6-311+G(d)

HOMO(eV)	LUMO(eV)	IP(eV)	EA(eV)	μ(eV)	χ(eV)	η(eV)	S(eV)	ω(eV)
-6.44	-3.63	6.44	3.63	-5.03	5.03	1.40	0.70	9.02

Table 5. Excitation energy (nm) and oscillator strength of P3OT at DFT/B3LYP/6-311+G(d)

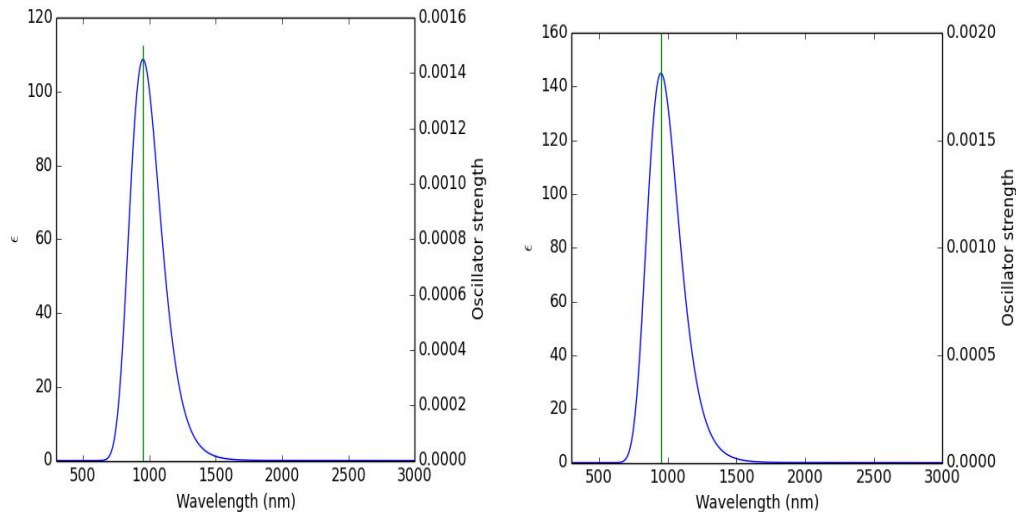| Model	PCM		C-PCM		IEFPCM	
Solvent	**Excitation Energy(nm)**	**Oscillator strength**	**Excitation Energy(nm)**	**Oscillator strength**	**Excitation Energy(nm)**	**Oscillator strength**
Chloroform	952.21	0.0020	952.66	0.0022	952.21	0.0020
THF	950.10	0.0020	951.36	0.0022	950.10	0.0020
Toluene	956.07	0.0020	955.89	0.0022	956.07	0.0020

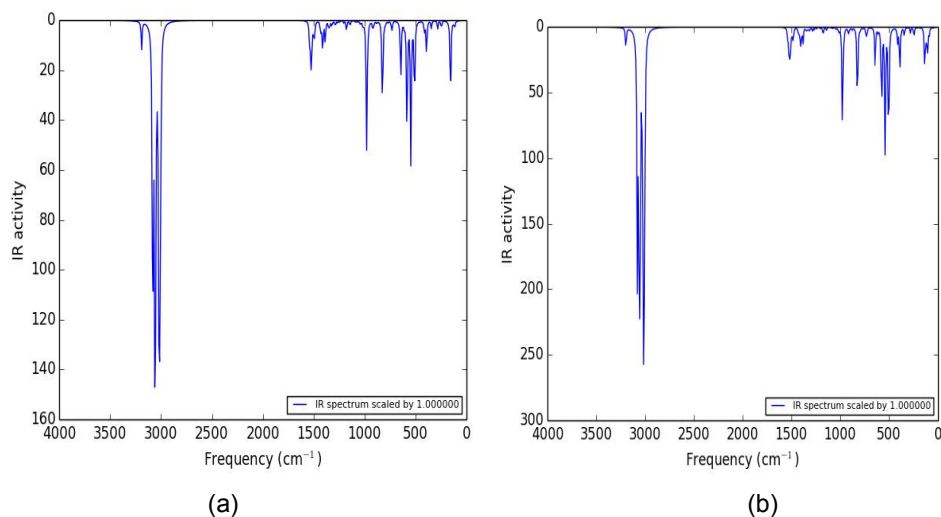**Fig. 3. UV-Visible Spectrum of P3OT (a) Vacuum (b) Medium**

Fig. 4. IR Spectrum of P3OT in (a) vacuum (b) medium

5. CONCLUSION

A DFT study was carried out to study the molecular and electronic properties of P3OT for solar cell application. The study reported the stability test and optimization at different basis sets: STO-3G, 3-21G, 6-31G, 6-311G, the ground state energy obtained at B3LYP/6-311G was found to be *-23566.8294eV*.The optimized parameters (bond length and bond angle) were calculated at DFT/B3LYP/6-311+G(d), the results obtained show that the lowest average value of bond length in vacuum and medium are *1.08311Å* and *1.0830Å* while the lowest value of the bond angle ranges from *105.429-105.815°* in vacuum and *105.449-105.923°* in a medium.

The HOMO, LUMO, and Energy gap are obtained as *-6.44eV, -3.63eV* and *2.81eV* in vacuum, while the results obtained in the medium shows a little effect on the HOMO,LUMO and energy gap for all the solvents. The energy-gap was compared with the ones in literature (2.51eV). The reported result was in agreement with the experimental value but is leading by 0.3eV.The ionization potential, electron affinity, chemical potential, electronegativity, hardness, softness and electrophilicity of the studied molecule were calculated and reported as *6.44eV, 3.63eV, -5.03eV, 5.03eV, 1.40eV, 0.70eV,* and *9.02eV*.This indicates the high stability and low

reactivity of the molecule in chemical reaction and also indicates that the studied molecule is a good electrophile. From the UV-VIS spectrum, the excitation energy and oscillator strength are found to be *948.46nm* and 0.0015 in the vacuum, while in the medium, the presence of solvents increases the excitation energy in the range *950.10-956.07nm* and oscillator strength of the molecule in the range *0.0020-0.0022*. This indicates that P3OT is a good photovoltaic material because of its strong absorption character in the visible and near-infrared regions. The result of the IR spectrum shows that the studied molecule was stable in both the vacuum and the medium since no imaginary frequency was observed. It was also observed that the most intense frequency was found to be *3062cm^{-1}* at an intensity of *111.70km/mol* in the vacuum and *3058cm^{-1}* at intensity of *190.69km/mol* in the medium. The theoretical value of the open-circuit voltage was found to be *2.711eV*, this value is sufficient for possible electron injection therefore poly (3-octylthiophene -2,5- diyl) can be used for solar cell application.

6. RECOMMENDATION

The authors recommend the study of the molecule in anionic and cationic forms to give further details of its properties for practical applications.

ACKNOWLEDGEMENTS

COMPETING INTERESTS

Authors have declared that no competing interests exist.

REFERENCES

1.   Edilene AS, Vinicius J, Rodrigues de O, Maria LB, Carlos's J, Leopoldo C, Clarissa de AO. poly(3-octylthiophene)/stearic acid Langmuir and Langmuir-blodgett films: preparation and characterization.
2.   Yen-Ju C, Sheng HY, Chain-Shu. H. Synthesis of conjugated polymer for organic solar cell applications. Chem Rev; 2009.
3.   Abu-Abdeen M. Ayman S. Ayesh, and Abdullah A. Aljaafari. Physical Characterizations of Semi Conducting conjugated polymer.CNT Nanocomposites. J Polymer Red; 2012.
4.   Ashkan S, Muhammad MS, Muhammad Y. Determination of HOMO and LUMO of [6,6]-Phenyl C$_{61}$-Butyric Acid 3-Ethylthiophene Ester and Poly (3-Octylthiophene-2,5-diyl). Sains Malaysiana. 2011;40(2): 173-176.
5.   Tatsuya D, Eisuke N, Fabrication of poly(3-octylthiophene-2,5-diyl) Electrochemiluminiscence (ECL) device assisted by perylene. Materials 2013;6:1704-1717.
6.   Natalia N, Piotr D, Dariusz M, and Janusz J,(2020). The determination of the electronic parameters of thin amorphous organic films by ellipsometric and spectrophotometric study. Coatings. 2020;10:980.
     DOI: 10.3390.
7.   Kalpana G. Lim A. Ekanayake P, Iskandar PM Cyanidin-Based Novel Organic Sensitizer for Efficient Dye-Sensitized Solar Cells: DFT/TDDFT Study. International Journal of Photo Energy; 2017.
     ID. 8564293.
8.   El Alamy A, Bourass M, Amina A, Mohammed H, Mohammed B. New organic dyes based on phenylenevinylene for solar cells: DFT and TD-DFT investigation. Karbala. International Journal of Mordern Science. 2017;3:75-82.
9.   Taoufik S, Bousselham K, Abbes L, Brahim A. Photovoltaic energy conversion and optical properties of organic molecule based on aceanthraquinoxaline. Der pharma chemical, 2017;9(2): 37-42.
10. Yuanchao L, Lu M, Haibin W, Yuanzuo L, Jianping L, Design, electron transfer process,and opto-electronic property of solar cell using triphenylamine-based D-☐-A architectures. Materials. 2019;12,193.
11. Bourass M, Benjelloun AT, Hamidi M, Benzakour M, Mcharfi M, Sfaira M, Serein- Spirau F, Lere-Porte JP, Sotiropoulos J.M, Bouzzine SM, Bouachrine M DFT Theoretical Investigation of ☐-Conjugated Molecules based on thienopyrazine and different acceptor moieties for Organic Photovoltaic Cells. Journal of Saudi Chemical Society. 2016;20:S415-S425.

12. Hachi M, El Khattabi S, Fitri A, Benjelloun AT. Benzekour M. Mcharfi M. Hamidi M. Bouachrine M, DFT & TD-DFT Studies of the ☐-Bridge Influence on the Photovoltaic Properties of dyes Based on Thieno [2,3-b]indole. J. Mater Environ. Sci.volume 2018;9:1200-1211.

13. Maylis O, Dimitrios A. Pantozis, Frank N. Density Functional Theory Photosynth. Res. 2009;102:443-453.

14. Ravindram P. Introduction to Density Functional Theory, Condensed Matter Physics; 2015.

15. Gidado A.S, Babaji B.G and Ado M Determination of vibrational frequencies, HOMO-LUMO Energy and IRspectra of Nucleobases (Adenine, Cytosine, Guanine Thymine and Uracil). J.NAMP 2015;31: 465-476.

16. Bendjeddou A, Tahar A, Abdelkrim G, Didier V Quantum chemical studies on molecular structure and stability descriptors of some *p* - Nitrophenyltetrathiafulvalenes by density functional theory (DFT). Acta Chim.Pharm.Indica: 2016;6(2):32-44. ISSN 2277-288X.

17. Abdulaziz H, Gidado AS, Musa A, Lawal. "Electronic structure and non linear optical properties of neutral and ionic pyrene and its derivatives based on density functional theory". J Mater. Sci. Rev. 2019;2(3):1-13

18. Frisch MJ, Trucks GW, Schlegel HB, Scuseria GE, Robb MA, Cheeseman JR, Scalmani G Barone V, Mennucci B, Peterson GA, Nakatsuji H, Caricato M, Li X, Hratchian HP, Izmaylov AF, Bloino J, Zheng G, Sonnenberg JL, Hada M, Ehara M, Toyotaz K, Fukuda R, Hasegawa J, Ishida M, Nakajima T, Honda Y, Kitao O, Nakai H, Vreven T, Montgomery JA, Jr, Peralta JE, Ogliaro F, Bearpark M, Heyd JJ, Brothers E, Kudin KN, Staroveror VN, Kobayashi R, Normand J, Raghavachari K, Rendell A, Burant JC, Iyengar SS, Tomasi J, Cossi M, Rega N, Millam JM, Klene M, Knox JE, Cross JB, Bakken V, Adamo C, Jaramillo J, Gomperts R, Stratmann RE, Yazyev O, Austin AJ, Cammi R, Pomelli C, Ochterski JW, Martin RL, Morokuma K, Zakrzewski VG, Voth GA, Salvador P, Dannenberg JJ, Dapprich S, Daniels AD, Farkas O, Foresman JB, Ortiz JV, Cioslowski J, Fox DJ. Gaussian 09, Revision 2009;A.1.

19. Mansur S, Yau D, Aliyu A, Tijjani RB, Abdullahi BA Computational Study of Lawsonia Inermis as potential and promising candidate for production of solar cell. European Journal of Advanced Chemistry Research; 2021. ISSN 2684-4478.

20. Shukla A, Rajendra PT Shukla KDP Electronic state properties; Bond length and Bond angle of phenol and its some derivatives. Int.J.Chem.Sci: 2011;9(2):627-636.

21. Rajalakshmi.K and Sharmila.S (2020). Spectroscopic studies and vibrational assignments, HOMO- LUMO, UV-VIS,NBO Analysis of Benzonitrile. International Journal of ChemTech Research.13(3):225-239.

22. Kumer A, Boshir A, Sharif M.A and Abdullah. A (2017). A theoretical study of Aniline and Nitrobenzene by computational overview. AJOPACS 38092, 4(2):1-12.

23. Lakhlifi T, Abram T, Chtita S, Bejjit L, Bouachrine M,(2014). Electronic and photovoltaic Properties of new materials based on 6-mono-substituted and 3,6-disubstituted acridines and their application to design novel materials for organic solar cells. Journal of Computational Methods in Molecular Design. 4(3):19-27.

24. O'Boyle NM, Tenderholt AL, Langner KM. GaussSum 03. J.Comp.Chem 2008;29:839-845.

25. Gidado AS, Abubakar M, Galadanci GSM. Geometry optimization and Vibrational frequencies of Tetracene molecule in gas phase and in methanol based on Density Functional Theory and Restricted Hartree Fock. Bayero Journal of Pure and Applied Science. 2017;10(1):18-31.

26. Wolf VH IR PAL V2.0, A table driving infrared Application; 2010. Available: Bhttp://home.kpn.nl/~vheeswijk

---

Peer-review history:
The peer review history for this paper can be accessed here:
https://www.sdiarticle4.com/review-history/70854